ChemComm

COMMUNICATION

View Article Online
View Journal | View Issue

Cite this: *Chem. Commun.*, 2016, 52, 12829

Received 12th August 2016,
Accepted 23rd September 2016

DOI: 10.1039/c6cc06644e

www.rsc.org/chemcomm

A hexameric $[Mn^{III}_{18}Na_6]$ wheel based on $[Mn^{III}_3O]^{7+}$ sub-units†

Maria Manoli,[a] Ross Inglis,[b] Stergios Piligkos,[c] Lan Yanhua,[d] Wolfgang Wernsdorfer,‡[d] Euan K. Brechin*[b] and Anastasios J. Tasiopoulos*[a]

A novel hexameric $[Mn^{III}_{18}Na_6]$ wheel-like aggregate consisting of $[Mn^{III}_3O]$ triangles is reported. It is the second highest nuclearity oxime-based Mn cluster, the largest member of the recently-developed family of molecular oligomers based on $[Mn^{III}_3O]$ triangles, and the only one with a wheel-like metal topology.

There is significant interest in the synthesis of large molecular aggregates due to their interesting physical properties and beautiful crystal structures.[1,2] One of the main goals in the area of molecular magnetism involves the development of new methods for the utilization of magnetically interesting compounds as building-blocks for the construction of large clusters and multi-dimensional coordination polymers.[2a,3] Despite the significant efforts to achieve this target, examples of such large clusters based on smaller magnetic clusters are still rather limited.[2a,4] Amongst the most common building-blocks in manganese coordination chemistry are the homovalent $[Mn^{III}_3(\mu_3\text{-}O)]^{7+}$ and heterovalent $[Mn^{III}_2Mn^{II}(\mu_3\text{-}O)]^{6+}$ oxo-centred metal triangles which are often found as the main structural components in large compounds with complex structures.[2,5] Efforts aimed at developing high nuclearity clusters based on $[Mn^{III}_3O]$ sub-units were intensified after the discovery of discrete $[Mn^{III}_3(\mu_3\text{-}O)]^{7+}$ clusters displaying ferromagnetic exchange interactions and single-molecule magnetism (SMM) behaviour,[6] the isolation of a family of $[Mn^{III}_6]$ SMMs that includes a member with a record energy barrier to magnetization reversal for transition metal SMMs,[7] and several other clusters displaying interesting magnetic properties originating from tightly linked $[Mn_3(\mu_3\text{-}O)]^{n+}$ triangles sharing one or more of their edges.[8] More recently there has been significant interest in the construction of oligomeric clusters consisting of covalently linked oxime-based $[Mn^{III}_3O]^{7+}$ building-blocks. These investigations have afforded some dimeric $[Mn_3]_2$ and tetrameric $[Mn_3]_4$ aggregates displaying tetrahedral or rectangular core topologies.[9]

We have been interested in the development of new synthetic methods for the construction of high nuclearity Mn clusters. One of these methods, that involves the combination of phenolic oximes with diols, has afforded two structurally impressive complexes that describe a $[Mn_{32}]$ double-decker wheel,[10a] and an 1-D coordination polymer containing a $[Mn_{40}]$ octagonal super-structure.[10b] We now report the synthesis, structure and magnetic behaviour of the hexameric $[Mn^{III}_3Na]_6$ molecular wheel $[Mn^{III}_{18}Na_6(\mu_3\text{-}O)_6(sao)_{18}Br_{12}(H_2O)_{18}(DMF)_6]$ (**1**) (sao^{2-} is the dianion of salicylaldoxime) which is the second largest oxime-based Mn cluster known to date, the largest member of the family of molecular oligomers based on $[Mn_3]$ triangles, and the only one with a wheel-like metal topology.

The reaction of $MnBr_2{\cdot}4H_2O$, 2-(hydroxymethyl)phenol (hpH_2) and $saoH_2$ in the presence of sodium cyanate (NaOCN) in a 1 : 1 : 1 : 1 molar ratio in a 4 : 1 MeCN/DMF solvent mixture leads to the formation of **1** in ~45% yield.§ The molecular structure§ of **1** (Fig. 1 and 2) contains a $[Mn^{III}_{18}Na_6]$ wheel-like cluster consisting of six crystallographically equivalent oxime-based $[Mn^{III}_3O]^{7+}$ triangles linked through six Na^+ ions. The $[Mn^{III}_3Na]$ repeat unit of **1** contains one oxo-centred triangular arrangement of three Mn^{III} ions and a Na^+ ion attached to it *via* the O-atoms of the sao^{2-} ligands, which occupy the edges of the triangle. The axial coordination sites of the Mn^{III} ions are occupied by one bridging H_2O molecule, and terminal Br^- ions (2), H_2O (2) and DMF (1) molecules. The Mn^{III} ions are hexa-coordinated with distorted octahedral coordination geometries and all display the expected Jahn–Teller (JT) axial elongation, with the JT axes being perpendicular to the plane of the $[Mn_3]$ triangle. Two μ_3-, one μ_4-sao^{2-}, and one bridging H_2O ligand connect each $[Mn^{III}_3O]$ triangle with two neighbouring Na^+ ions, which in turn are linked to the next

[a] *Department of Chemistry, University of Cyprus, 1678 Nicosia, Cyprus. E-mail: atasio@ucy.ac.cy; Fax: +357 22895451; Tel: +357 22892765*
[b] *EaStCHEM School of Chemistry, The University of Edinburgh, David Brewster Road, Edinburgh, EH9 3FJ, UK. E-mail: E.Brechin@ed.ac.uk*
[c] *Department of Chemistry, University of Copenhagen, Universitetsparken 5, Copenhagen, Denmark*
[d] *Institut Néel, CNRS, BP-166, Grenoble Cedex 9, France*

† Electronic supplementary information (ESI) available: Experimental details, structural figures and TGA data. CCDC 1498633. For ESI and crystallographic data in CIF or other electronic format see DOI: 10.1039/c6cc06644e

‡ Current address: KIT, Physikalisches Institut, Wolfgang-Gaede-Str. 1D-76131 Karlsruhe, Germany.

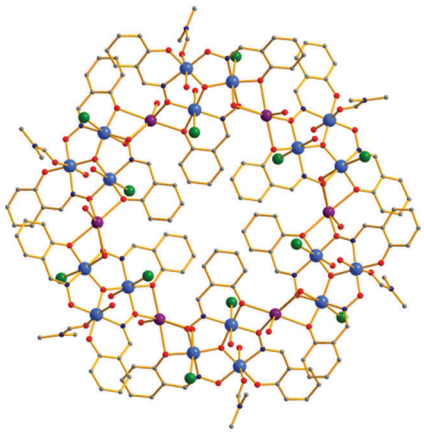

Fig. 1 Representation of the molecular structure of **1**. Colour code: Mn blue; Na, purple; Br, green; O, red; N, dark blue; C, grey. H atoms are omitted for clarity.

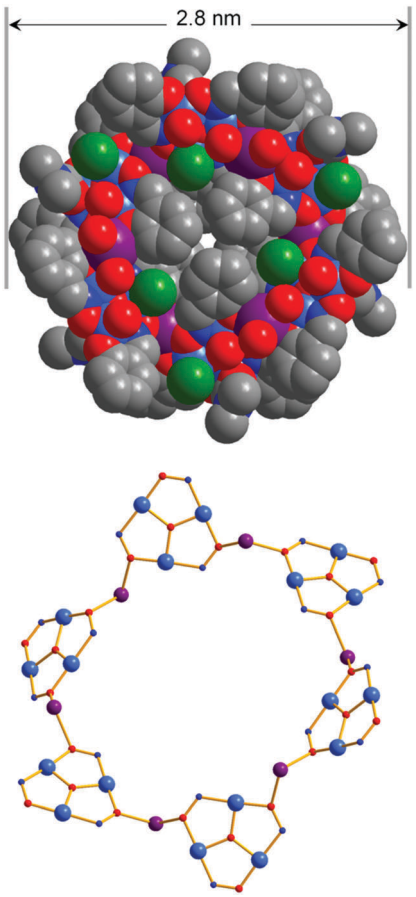

Fig. 2 Space-filling representation of the molecular structure of **1**, emphasizing its nano-sized dimensions (top). The structural core of **1** highlighting the [Mn_3] triangles linked through Na^+ ions (bottom). Colour code: Mn, blue; Na, purple; Br, green; O, red; N, dark blue; C, grey. H atoms are omitted for clarity.

$[Mn^{III}_3O]$ sub-units forming the $[Mn_{18}Na_6]$ wheel. Two sao^{2-} ligands bridge in a $\eta^1{:}\eta^1{:}\eta^2{:}\mu_3$-mode to two Mn^{III} ions and one Na^+ ion, and one bridges in a $\eta^2{:}\eta^1{:}\eta^2{:}\mu_4$-fashion to two Mn^{III} and two Na^+ ions. The phenyl rings of twelve of the sao^{2-} ligands are located outside the $[Mn_{18}Na_6]$ wheel, whereas those of the remaining six occupy the central cavity creating a hydrophobic shell (Fig. 2, top). The Mn–O–N–Mn torsion angles are rather small, ranging from 6.4 to 12.9°, in agreement with the values observed for other sao^{2-}-based $[Mn^{III}_3O]$ triangles.[6,7] The neighbouring $[Mn^{III}_3O]$ sub-units are significantly tilted as revealed from the angle between the planes defined by the Mn^{3+}/O^{2-} ions of adjacent $[Mn^{III}_3O]$ units which is ~52.2° (Fig. 2, bottom). As a result the aggregate of **1** deviates significantly from planarity. The $[Mn^{III}_3O]$ triangles are well separated from each other, the shortest inter-triangle Mn···Mn distance being ~6.23 Å. Complex **1** is of nano-sized dimensions with an outer diameter of ~2.8 nm (Fig. 2, top) and a thickness of ~0.8 nm. Clearly, complex **1** is a large cluster and indeed is one of the largest oxime-based Mn complexes known, being smaller only than the $[Mn_{32}]$ double-decker wheel.[10a] Close examination of the packing of **1** reveals a parallel arrangement of $[Mn_{18}Na_6]$ molecules in the crystal and the formation of columns running along the *c*-axis of the cell (Fig. S1, ESI†).

The direct current (dc) molar magnetic susceptibility, χ (where $\chi = M/B$; and M is the magnetization), of polycrystalline **1**·3DMF·30H_2O was measured in an applied magnetic field, B, of 0.1 T, over the 5–300 K temperature range. The data is plotted in Fig. 3 per $[Mn^{III}_3]$ triangle. At room temperature, the χT product of **1** is 7.8 $cm^3\ mol^{-1}$ K. This value is lower than that expected from the spin-only contribution to the magnetism of a Mn^{III} trinuclear unit (9.0 $cm^3\ mol^{-1}$ K, with g_{Mn} = 2.00), assuming that the magnetic properties of **1** arise as the superposition of the magnetic properties of six non-interacting $[Mn^{III}_3]$ units. Upon cooling, the χT product decreases continuously to reach 2.5 $cm^3\ mol^{-1}$ K per $[Mn^{III}_3]$ at T = 5 K. This behaviour is indicative of antiferromagnetic interactions within the $[Mn^{III}_3]$ units. To better define the magnetic properties of **1**, variable-temperature-and-variable-field (VTVB) magnetization data were collected in the field range 0.5–7.0 T and in the temperature range 2–7 K. These data are shown as M/μ_B *versus* $\mu_B B/kT$ in the inset of Fig. 3.

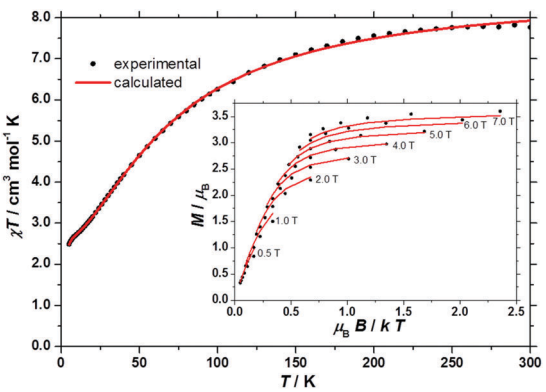

Fig. 3 χT product of **1** *versus* T plotted per $[Mn^{III}_3]$ triangle. Inset: Variable temperature-and-variable-field (VTVB) magnetization data of **1** in the field range 0.5 to 7.0 T and in the temperature range 2 to 7 K. The experimental data are shown as black circles. The calculated curves, obtained from full matrix diagonalization of spin-Hamiltonian (1) for isolated Mn^{III}_3 triangles, are shown as solid red lines.

For the interpretation of the magnetic properties of **1**, we consider that they arise as a superposition of the magnetic properties of six non interacting $[Mn_3^{III}]$ units. Thus, we used spin-Hamiltonian (1):

$$\hat{H} = \sum_{i,j\geq i} -2J_{ij}\hat{S}_i \cdot \hat{S}_j + \mu_B B g_{Mn} \sum_i \hat{S}_i + \sum_i D_i\left[\hat{S}_i^2 - S(S+1)/3\right] \quad (1)$$

with i, j running over all Mn^{III} centres of a $[Mn_3^{III}]$ unit, J the isotropic magnetic exchange interaction between Mn^{III} centres, $\hat{S}$ a spin-operator, μ_B the Bohr magneton, B the applied magnetic field, $g_{Mn} = 2$, the isotropic g-factor common to all Mn^{III} centres, D the axial magnetic anisotropy of Mn^{III}, and $S = 2$. Taking into consideration the crystal structure of **1**, we use in our model three distinct exchange interaction parameters (J_{12}, J_{23}, J_{13}) reflecting the scalene nature of the triangular $[Mn_3^{III}]$ units. The experimental χT product and VTVB magnetization data were numerically fitted to spin-Hamiltonian (1) by use of the simplex algorithm.[11] This resulted in the following best-fit parameters: $J_{12} = -6.35$ cm^{-1}, $J_{23} = -2.22$ cm^{-1}, $J_{13} = -0.85$ cm^{-1} and $D_{Mn} = -2.0$ cm^{-1}. The three different best-fit exchange parameter values can be correlated to the three different Mn–N–O–Mn torsion angles in the $[Mn_3^{III}]$ units, which are smallest between Mn1 and Mn2 and largest between Mn1 and Mn3. The best-fit curves are shown as solid red lines in Fig. 3. Neglecting the Mn^{III} anisotropy, the ground spin-state is an $S = 2$ state separated by approximately 9 cm^{-1} from the first excited spin state, which is an $S = 1$ state. This is in agreement with previous studies on analogous, isolated $[Mn_3O(sao)_3]^+$ triangles with similar torsion angles.[6,7a,b,12] Single crystal hysteresis loop measurements on complex **1** show no sign of SMM behaviour, even to temperatures as low as 30 mK (Fig. S3, ESI†).

Concluding, an aesthetically pleasing nano-sized hexameric wheel-like cluster containing oxime-based $[Mn_3^{III}(\mu_3\text{-}O)]^{7+}$ sub-units is reported. It is the largest member of the recently-developed family of molecular oligomers consisting of $[Mn_3^{III}]$ triangles and the only one with a wheel-like metal topology.[9] Complex **1** is also the only oxime-based $[Mn_3^{III}]_n$ ($n > 2$) molecular oligomer where the sub-units are connected *via* a diamagnetic metal ion; in all other oligomeric complexes they are linked through bulky organic ligands. Because the Na^+ ions are intimately associated with the $[Mn_3^{III}]$ triangles, **1** can also be described as a heterometallic $[M_{24}]$ cluster, being the second-largest oxime-containing Mn cluster reported to date. This compound was prepared by a method involving the use of a combination of a phenolic oxime with a diol in reactions with Mn salts, although only the oxime appears in the final product, as was also the case for the largest known oxime – based Mn cluster, the Mn_{32} double-decker wheel.[10a] Reactions repeated without the diol present do not form **1**. Clearly this synthetic method is proving invaluable for the isolation of high nuclearity clusters. Further investigations are in progress targeting $[Mn_{18}Na_6]$ analogues with different oximes and alternative [diamagnetic and paramagnetic] connecting metals ions. The formation of complex **1** therefore opens up new avenues in the roadmap of molecular oligomers based on $[Mn_3^{III}]$ triangles that should provide access to structurally and magnetically novel complexes.

This work was supported by the Cyprus Research Promotion Foundation Research Grant "ΑΝΑΒΑΘΜΙΣΗ/ΠΑΓΙΟ/0308/12" which is co-funded by the Republic of Cyprus and the European Regional Development Fund. We also thank the University of Cyprus for an internal research grant to AJT. EKB thanks the Villum Foundations (Denmark) for a Velux Visiting Professorship.

Notes and references

§ The diol does not appear in the final product, but its presence in the reaction mixture is essential for the formation of **1**. Vacuum-dried solid analysed (C, H, N) as **1**·3DMF·30H_2O (see also Fig. S2 and the corresponding discussion in ESI†). Calcd (found): C 29.95 (29.85), H 4.09 (3.75), N 6.16 (6.41). Crystal data for **1**: $C_{144}H_{168}Br_{12}Mn_{18}N_{24}Na_6O_{66}$, $M = 5334.47$, trigonal, $a = b = 44.310(2)$ Å, $c = 21.224(1)$ Å, $V = 36088(2)$ Å^3, $T = 100(2)$ K, space group $R\bar{3}c$, $Z = 6$, $\rho_{calcd} = 1.473$ g cm^{-3}, 24 939 reflections collected, 7153 reflections used ($R_{int} = 0.0357$), R_1 [$I > 2\sigma(I)$] = 0.0688, wR_2 (all data) = 0.2175. The asymmetric unit also contains severely disordered solvent molecules that could not be modeled properly. Thus, the SQUEEZE program was used to eliminate the contribution of the electron density in the disordered solvent region from the overall intensity data.

1 (*a*) C. J. Milios and R. E. P. Winpenny, *Struct. Bonding*, 2015, **164**, 1; (*b*) R. Bagai and G. Christou, *Chem. Soc. Rev.*, 2009, **38**, 1011; (*c*) D. Gatteschi and R. Sessoli, *Angew. Chem., Int. Ed.*, 2003, **42**, 268; (*d*) Y.-Z. Zheng, G.-J. Zhou, Z. Zheng and R. E. P. Winpenny, *Chem. Soc. Rev.*, 2014, **43**, 1462; (*e*) M. Nakano and H. Oshio, *Chem. Soc. Rev.*, 2011, **40**, 3239; (*f*) X.-Y. Wang, C. Avendano and K. R. Dunbar, *Chem. Soc. Rev.*, 2011, **40**, 3213; (*g*) G. Aromí, D. Aguila, P. Gamez, F. Luis and O. Roubeau, *Chem. Soc. Rev.*, 2012, **41**, 537.

2 (*a*) C. Papatriantafyllopoulou, E. E. Moushi, G. Christou and A. J. Tasiopoulos, *Chem. Soc. Rev.*, 2016, **45**, 1597; (*b*) G. E. Kostakis, A. M. Ako and A. K. Powell, *Chem. Soc. Rev.*, 2010, **39**, 2238; (*c*) A. Escuer, J. Esteban, S. P. Perlepes and T. C. Stamatatos, *Coord. Chem. Rev.*, 2014, **275**, 87; (*d*) S. P. Watton, P. Fuhrmann, L. E. Pence, A. Ganeschi, A. Cornia, G. L. Abbati and S. J. Lippard, *Angew. Chem., Int. Ed. Engl.*, 1997, **36**, 2774; (*e*) G. L. Abbati, A. Cornia, A. C. Fabretti, A. Ganeschi and D. Gatteschi, *Inorg. Chem.*, 1998, **37**, 1430; (*f*) G. L. Abbati, A. Cornia, A. C. Fabretti, W. Malavasi, L. Schenetti, A. Ganeschi and D. Gatteschi, *Inorg. Chem.*, 1997, **36**, 6443.

3 I.-R. Jeon and R. Clérac, *Dalton Trans.*, 2012, **41**, 9569.

4 (*a*) M. Manoli, S. Alexandrou, L. Pham, G. Lorusso, W. Wernsdorfer, M. Evangelisti, G. Christou and A. J. Tasiopoulos, *Angew. Chem., Int. Ed.*, 2016, **55**, 679; (*b*) M. Charalambous, E. E. Moushi, C. Papatriantafyllopoulou, W. Wernsdorfer, V. Nastopoulos, G. Christou and A. J. Tasiopoulos, *Chem. Commun.*, 2012, **48**, 5410.

5 (*a*) E. K. Brechin, *Chem. Commun.*, 2005, 5141; (*b*) A. J. Tasiopoulos and S. P. Perlepes, *Dalton Trans.*, 2008, 5537.

6 (*a*) R. Inglis, S. M. Taylor, L. F. Jones, G. S. Papaefstathiou, S. P. Perlepes, S. Datta, S. Hill, W. Wernsdorfer and E. K. Brechin, *Dalton Trans.*, 2009, 9157–9168 and references therein; (*b*) C. J. Milios, R. Inglis, L. F. Jones, A. Prescimone, S. Parsons, W. Wernsdorfer and E. K. Brechin, *Dalton Trans.*, 2009, 2812–2822; (*c*) T. C. Stamatatos, D. Foguet-Albiol, C. C. Stoumpos, C. P. Raptopoulou, A. Terzis, W. Wernsdorfer, S. P. Perlepes and G. Christou, *J. Am. Chem. Soc.*, 2005, **127**, 15380; (*d*) J. Cano, T. Cauchy, E. Ruiz, C. J. Milios, C. C. Stoumpos, T. C. Stamatatos, S. P. Perlepes, G. Christou and E. K. Brechin, *Dalton Trans.*, 2008, 234.

7 (*a*) R. Inglis, C. J. Milios, L. F. Jones, S. Piligkos and E. K. Brechin, *Chem. Commun.*, 2012, **48**, 181; (*b*) C.-I. Yang, Z.-Z. Zhang and S.-B. Lin, *Coord. Chem. Rev.*, 2015, **289–290**, 289; (*c*) C. J. Milios, A. Vinslava, W. Wernsdorfer, S. Moggach, S. Parsons, S. P. Perlepes, G. Christou and E. K. Brechin, *J. Am. Chem. Soc.*, 2007, **129**, 2754.

8 (*a*) A. Escuer, B. Cordero, M. Font-Bardia, S. J. Teat and O. Roubeau, *Eur. J. Inorg. Chem.*, 2016, 1232; (*b*) R. Vicente, M. S. El Fallah, B. Casanovas, M. Font-Bardia and A. Escuer, *Inorg. Chem.*, 2016, **55**, 5735.

9 (*a*) T. N. Nguyen, W. Wernsdorfer, K. A. Abboud and G. Christou, *J. Am. Chem. Soc.*, 2011, **133**, 20688; (*b*) A. M. Mowson, T. N. Nguyen, K. A. Abboud and G. Christou, *Inorg. Chem.*, 2013, **52**, 12320; (*c*) J. M. Frost,

S. Sanz, T. Rajeshkumar, M. B. Pitak, S. J. Coles, G. Rajaraman, W. Wernsdorfer, J. Schnack, P. J. Lusby and E. K. Brechin, *Dalton Trans.*, 2014, **43**, 10690; (*d*) T. N. Nguyen, M. Shiddiq, T. Ghosh, K. A. Abboud, S. Hill and G. Christou, *J. Am. Chem. Soc.*, 2015, **137**, 7160; (*e*) T. N. Nguyen, W. Wernsdorfer, M. Shiddiq, K. A. Abboud, S. Hill and G. Christou, *Chem. Sci.*, 2016, **7**, 1156.

10 (*a*) M. Manoli, R. Inglis, M. J. Manos, V. Nastopoulos, W. Wernsdorfer, E. K. Brechin and A. J. Tasiopoulos, *Angew. Chem., Int. Ed.*, 2011, **50**, 4441; (*b*) M. Manoli, R. Inglis, M. J. Manos, G. S. Papaefstathiou, E. K. Brechin and A. J. Tasiopoulos, *Chem. Commun.*, 2013, **49**, 1061.

11 H. Press, S. A. Teukolsky, W. T. Vetterling and B. P. Flannery, *Numerical Recipes in C: The Art of Scientific Computing*, Cambridge University Press, Cambridge, 2nd edn, 1992.

12 E. Manolopoulou, C. C. Stoumpos, M. Siczek, T. Lis, E. K. Brechin and C. J. Milios, *Eur. J. Inorg. Chem.*, 2010, 483.